Monthly Notices
of the
ROYAL ASTRONOMICAL SOCIETY

Mon. Not. R. Astron. Soc. **415,** 1523–1526 (2011) doi:10.1111/j.1365-2966.2011.18796.x

Timing and X-ray spectral features of *Swift* J1626.6−5156

Burçin İçdem,[1]★ Sıtkı Çağdaş İnam[2]★ and Altan Baykal[1]

[1]*Department of Physics, METU, Ankara 06531, Turkey*
[2]*Department of Electrical and Electronics Engineering, Başkent University, Ankara 06530, Turkey*

Accepted 2011 March 25. Received 2011 March 22; in original form 2011 January 26

ABSTRACT

In this paper, we extend the timing analysis by Baykal et al. of *Swift* J1626.6−5156 using *RXTE*–PCA observations between MJD 53724 and MJD 55113 together with a *Chandra*–ACIS observation on MJD 54897 with a 20-ks exposure. We also present the X-ray spectral analysis of these *RXTE* and *Chandra* observations. We find that the spin-up rate of the source is correlated with the X-ray flux. Using this correlation, we estimate the distance and surface magnetic field of the source as ∼15 kpc and $\sim 9 \times 10^{11}$ G, respectively. From the spectral analysis, we find that the power-law index increases and hydrogen column density decreases with a decreasing flux.

Key words: accretion, accretion discs – stars: neutron – pulsars: individual: *Swift* J1626.6−5156 – X-rays: binaries.

1 INTRODUCTION

Swift J1626.6−5156 is a transient accretion-powered pulsar with a spin period of ∼15 s (Markwardt & Swank 2005; Palmer et al. 2005). It was first detected on 2005 December 18 with the *Swift* Burst Alert Telescope (BAT) (Palmer et al. 2005). Shortly after the 2005 outburst of the source, Reig et al. (2008) observed two X-ray flares with a duration of ∼450 s each, during which the pulsed fraction increased up to ∼70 per cent. After the flares, the average count rate and the pulsed fraction were restored quickly to their pre-flare values. Reig et al. (2008) also reported a weak QPO feature with a characteristic frequency of 1 Hz and a fractional rms of 4.7 per cent.

The proposed optical companion of the source (2MASS16263652−5156305, USNO-B1.0 0380−0649488) was found to show strong Hα emission, which indicates that it is a Be star (Negueruela & Marco 2006). As the infrared magnitudes of the companion are rather large for a Be star, i.e. the star is unusually faint in the infrared band ($J = 13.5$, $H = 13$, $K = 12.6$; Rea et al. 2006), *Swift* J1626.6−5156 is thought to be an unusual Be/X-ray binary system.

Baykal, Gogus & Inam (2010) studied the long-term monitoring *RXTE* (Rossi X-ray Timing Explorer) – PCA (Proportional Counter Array) observations of the source between MJD 53724 and 54410. They obtained timing solution of the source and found the orbital period to be 132.89 d. Baykal et al. (2010) also constructed long-term pulse-frequency history of *Swift* J1626.6−5156 and showed that the time-scale of the X-ray modulations varied, which led to earlier suggestions (Reig et al. 2008; DeCesar, Pottschmidt & Wilms 2009) of orbital periods at about one-third and one-half of the orbital period of *Swift* J1626.6−5156.

In this article, we extend the timing studies of Baykal et al. (2010) by including the analysis of *RXTE*–PCA observations between MJD 54410 and MJD 55113 and a *Chandra*–ACIS observation with a 20-ks exposure on MJD 54897. We also present X-ray spectral analysis of these *RXTE* and *Chandra* observations. In the next section, we describe the observations. In Sections 3 and 4, we present our timing and X-ray spectral analysis. In Section 5, we discuss our results.

2 OBSERVATIONS

We analysed the data from PCA on board *RXTE* (Jahoda et al. 1996) of *Swift* J1626.6−5156 between MJD 53724 and MJD 55113 with a total exposure of ∼449 ks, divided into 411 observations with exposures between ∼1 and ∼2 ks. We also note that this work includes a more detailed analysis of the *RXTE*–PCA data between MJD 53724 and 54410 which were used before by Baykal et al. (2010).

The *RXTE*–PCA is an array of five Proportional Counter Units (PCUs) sensitive to the 2–60 keV energy range, with a total effective area of ∼7000 cm^2 and a field of view of ∼1° full width at half-maximum (FWHM). During the analysed *RXTE*–PCA observations, the number of active PCUs varied between one and four. Before MJD 53964, there were 1–2 ks long observations every 2–3 d. After MJD 53964, observations were sampled in pairs, containing two consecutive 1–2 ks long observations separated by ∼0.3–0.6 d. The two observations in each of these pairs were separated from each other by ∼9–10 d. In the timing analysis, we used all the available layers of PCUs. For the spectral analysis, we used the layers of PCU2 only.

★E-mail: burcinm@astroa.physics.metu.edu.tr (BI); inam@baskent.edu.tr (SCI)

In addition to the *RXTE*–PCA data, we also used a *Chandra* AXAF CCD Imaging Spectrometer (ACIS; Garmire et al. 2003) observation of *Swift* J1626.6−5156 on MJD 54897 with an exposure of 20 ks. This observation contains ACIS-S FAINT TE (timed exposure) mode data.

3 TIMING ANALYSIS

For the timing analysis, we used 3–20 keV *RXTE*–PCA light curves with a time resolution of 0.375 s, which were generated from the PCA GoodXenon data. These light curves were background subtracted with the standard PCA analysis tools (pcabackest in HEASOFT) using the background estimator models of the *RXTE* team. The arrival times were corrected to the barycentre of the Solar system.

A pulse timing analysis between MJD 53724 and 54410 was already performed and the corresponding pulse frequencies were obtained by Baykal et al. (2010). In this work, we extended this analysis which is based on the cross-correlation of pulse profiles represented harmonically (Deeter & Boynton 1985) to the data between MJD 54410 and 55113. We were not able to obtain pulse frequencies using the cross-correlation technique for the data after MJD ∼54750 since the pulse profiles obtained for these data were found to be statistically insignificant. In Fig. 1 we present the extended pulse frequency evolution of *Swift* J1626.6−5156. The pulse frequencies in Fig. 1 were orbitally corrected using the orbital model of the source found by Baykal et al. (2010).

We extracted a 20 ks long light curve of the source from *Chandra*–ACIS observation on MJD 54897 with a time resolution of 0.44 s. Cross-correlating the eight pulse profiles obtained from the ∼2.5 ks long segments of the *Chandra*–ACIS observation with a template pulse obtained from the whole observation, we obtained the spin period of the *Swift* J1626.6−5156 to be $(6.520\,59 \pm 0.000\,75) \times 10^{-2}$ Hz. We obtained 0.3–8 keV pulse profiles of the source by folding of the whole *Chandra*–ACIS light curve with this frequency (see Fig. 2).

By a linear fitting of consecutive pulse frequencies with a timespan of ∼10–140 d, we obtained pulse frequency derivatives of the source between MJD 53724 and 54750. In Fig. 3, we present these frequency derivatives as a function of the corresponding 3–20 keV unabsorbed flux values.

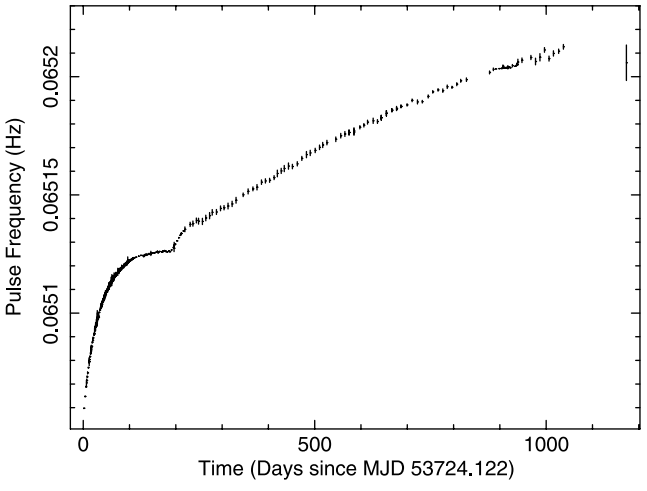

Figure 1. The pulse frequency evolution of *Swift* J1626.6−5156 after correcting for the binary orbital motion. The rightmost point corresponds to the *Chandra*–ACIS observation.

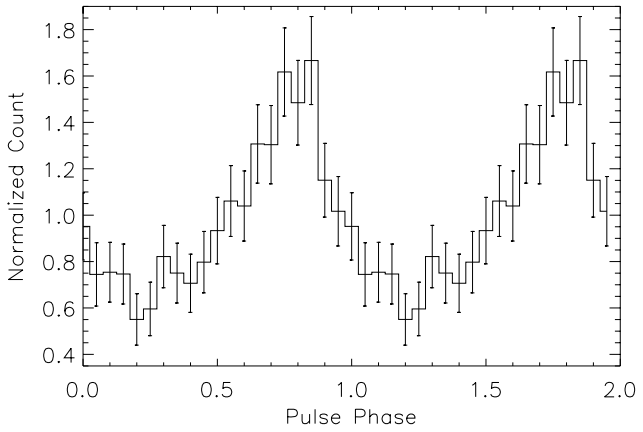

Figure 2. 0.3–8 keV pulse profile obtained from the *Chandra*–ACIS observation.

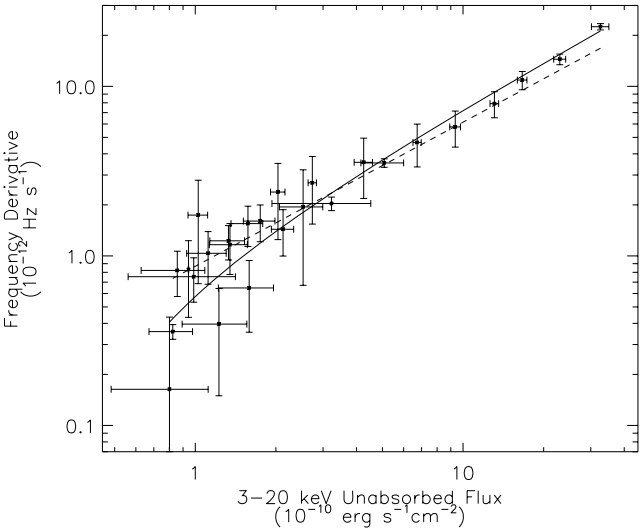

Figure 3. The frequency derivative of *Swift* J1626.6−5156 as a function of 3–20 keV unabsorbed X-ray flux obtained from the *RXTE*–PCA observations. The solid and dashed lines correspond to the torque models with and without dimensionless torque parameter, respectively.

4 SPECTRAL ANALYSIS

In order to calculate the 3–20 keV unabsorbed X-ray flux values of the source, we obtained X-ray spectra from the *RXTE*–PCA observations corresponding to the spin frequency derivative measurements. We used the Standard-2 mode data, providing 128 channel spectra at 16-s time resolution. Spectrum, background and response matrix files were created using the FTOOLS 6.9 data analysis software. Energy channels corresponding to the 3–20 keV energy range were used to fit the spectra. We ignored photon energies lower than 3 keV and higher than 20 keV, and added 0.6 per cent systematic error to the errors (see Wilms et al. 1999; Coburn et al. 2000). Using *Chandra*–ACIS data, we also obtained 0.3–8 keV X-ray spectrum of the source (see Table 1).

To fit the X-ray spectra, we used an absorbed power-law model with a high-energy cut-off expressed as $e^{(E_C-E)/E_F}$ where E_C is the cut-off energy and E_F is the e-fold energy (see White, Swank & Holt 1983). In addition to this model, iron line complex was modelled as a Gaussian, peaking at ∼6.5 keV. We could not resolve Cyclotron

Table 1. X-ray spectral parameters of *Swift* J1626.6−5156 (errors indicate the 1σ confidence level).

Instrument	*RXTE*–PCA	*RXTE*–PCA	*RXTE*–PCA	*Chandra*–ACIS
Time interval (MJD–MJD)	53724–53901	53901–54751	54751–55113	54897.31–54897.56
Exposure (ks)	227	175	47	20
$n_{\rm H}$ (10^{22} cm^{-2})	6.31 ± 1.31	1.21 ± 0.76	0.50 (fixed)	0.83 ± 0.11
Power-law index	1.90 ± 0.09	2.00 ± 0.05	2.46 ± 0.07	0.94 ± 0.12
Power-law norm. (10^{-2} photons keV^{-1} cm^2 s^{-1} at 1 keV)	37.4 ± 8.6	6.43 ± 0.82	1.00 ± 0.10	$(6.93 \pm 2.26) \times 10^{-3}$
Iron line peak (keV)	6.32 ± 0.39	6.57 ± 0.11	6.57 ± 0.09	6.58 (fixed)
Iron line sigma (keV)	1.40 ± 0.23	0.76 ± 0.12	0 (fixed)	0 (fixed)
Iron line norm. (10^{-4} photons cm^{-2} s^{-1})	66.8 ± 32.0	7.41 ± 2.41	0.68 ± 0.19	$(2.08 \pm 0.30) \times 10^{-2}$
Cut-off energy (keV)	12.4 ± 0.3	15.4 ± 0.5	16.1 (fixed)	–
E-fold energy (keV)	21.7 ± 2.4	10.1 ± 2.1	8.47 (fixed)	–
Energy range (keV–keV)	3–20	3–20	3–20	0.3–8
Unabsorbed X-ray flux (10^{-10} erg s^{-1} cm^{-2})	14.1 ± 0.1	1.97 ± 0.02	0.13 ± 0.04	$(9.43 \pm 1.26) \times 10^{-3}$
Reduced χ^2 / d.o.f.	1.42 / 32	1.47 / 32	0.61 / 36	1.25 / 34
Systematic error	0.6 per cent	0.6 per cent	0.6 per cent	–

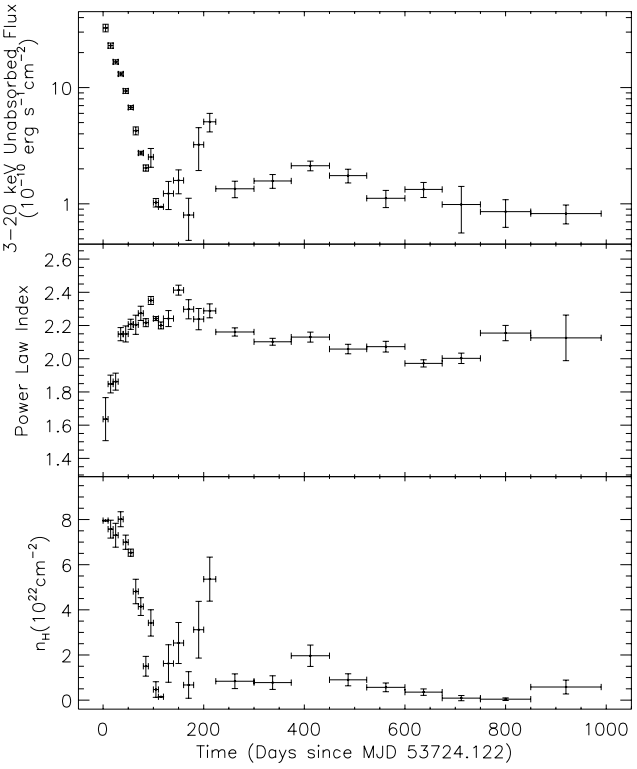

Figure 4. Temporal variations of 3–20 keV unabsorbed X-ray flux, power-law index and hydrogen column density.

lines of the source around ∼10–20 keV as suggested by Coburn et al. (2006). The temporal variations of the unabsorbed X-ray flux, power-law index and hydrogen column density are presented in Fig. 4. The averages of the cut-off energy and e-fold energy values were found to be ∼15 and ∼10 keV, respectively. To demonstrate the long-term spectral evolution of the source, we also constructed three long-term *RXTE*–PCA spectra of the source (see Table 1).

5 DISCUSSION

In Fig. 3, we show that *Swift* J1626.6−5156 is an accretion-powered pulsar that exhibits a correlation between spin-up rate and X-ray flux. Likewise, there are other accretion-powered pulsars that exhibit correlation between spin-up rate and X-ray flux: EXO 2030+375 (Parmar, White & Stella 1989; Wilson et al. 2002); A 0535+26 (Finger, Wilson & Harmon 1996b; Bildsten et al. 1997); 2S 1417−62 (Finger, Wilson & Chakrabarty 1996a; Inam et al. 2004); GRO J1744−28 (Bildsten et al. 1997); GRO J1750−27 (Scott et al. 1997); 2S 1845−024 (Finger et al. 1999); XTE J1543+568 (in't Zand, Corbet & Marshall 2001); SAX J2103.5+4545 (Baykal, Stark & Swank 2002; Baykal et al. 2007); and XMMU J054134.7−682550 (Inam et al. 2009).

The correlation between spin-up rate and X-ray flux can be considered as a sign of an accretion disc around a neutron star. In case of accretion via accretion disc, the Keplerian rotation of the disc is disrupted by the magnetosphere at the inner edge of the disc. Inside this radius, plasma is forced to move along the magnetic field lines to the magnetic poles of the neutron star. In case the effect of radiation pressure is negligible (i.e. source luminosity is much smaller than Eddington luminosity and/or polar cap radiation is not directly beamed on to the accretion disc), the value of inner disc radius (r_0) is primarily related to the balance between the magnetic pressure and the material pressure exerted by the accreted material. Thus the inner disc radius is expected to decrease with an increasing mass accretion rate ($\dot{M}$) and neutron star's mass (M) and a decreasing magnetic moment ($\mu \simeq BR^3$, where B is the surface magnetic field strength and R is the neutron star radius). These dependences may approximately be expressed as (Pringle & Rees 1972; Lamb, Pethick & Pines 1973)

$$r_0 = K\mu^{4/7}\,(GM)^{-1/7}\,\dot{M}^{-2/7}, \quad (1)$$

where G is the gravitational constant and K is a parameter that is of the order of unity. If K equals 0.91, r_0 corresponds to Alfvén radius for spherical accretion. The net torque exerted on the neutron star is estimated as (Ghosh & Lamb 1979)

$$2\pi I\,\dot{\nu} = n(\omega_{\rm s})\dot{M} l_K, \quad (2)$$

where I is the moment of inertia of the neutron star; $l_K = (GMr_0)^{1/2}$ is the specific angular momentum added by the Keplerian disc to

the neutron star at r_0;

$$n(\omega_s) \simeq 1.4(1-\omega_s/\omega_c)/(1-\omega_s) \quad (3)$$

is the dimensionless torque parameter which is a measure of the total (magnetic and material) torque exerted on the neutron star as a function of the fastness parameter,

$$\omega_s = \nu/\nu_K(r_0) = (r_0/r_{co})^{3/2} = 2\pi K^{3/2} P^{-1} (GM)^{-5/7} \mu^{6/7} \dot{M}^{-3/7}, \quad (4)$$

where $r_{co} = [GM/(2\pi\nu)^2]^{1/3}$ is the corotation radius at which the stellar angular velocity equals Keplerian angular velocity. In equation (3), ω_c is the critical fastness parameter which has been estimated as ∼0.35 (Ghosh & Lamb 1979; Wang 1987; Ghosh 1993; Li & Wickramasinghe 1998; Torkelsson 1998; Dai & Li 2006).

The accretion leads to X-ray emission from the neutron star surface with the luminosity

$$L = \eta \frac{GM\dot{M}}{R}, \quad (5)$$

where $\eta \leq 1$ is the efficiency factor. From equations (1), (2) and (5), the spin-up rate is estimated as

$$\dot{\nu} \propto n(\omega_s) L^{6/7} = n(\omega_s)(4\pi d^2 F)^{6/7}, \quad (6)$$

where d is the distance to the source and F is the X-ray flux. If the dimensionless torque $[n(\omega_s)]$ is set to unity, this is the case in which material torques dominate. If the dimensionless torque is not unity, i.e. if it is calculated using equation (3), then this corresponds to the case in which magnetic torques are not negligible. In Fig. 3, we present fits with $n = 1$ and the case for which the dimensionless torque is not unity (solid lines). We found that the model including non-unity dimensionless torque gives a better fit with a reduced χ^2 of 1.05 compared to the fit with the unity dimensionless torque giving a reduced χ^2 of 6.14.

Using equation (6) and Fig. 3, we estimated the distance to the source as ≃15 kpc. This leads to a surface magnetic field estimate of $\simeq 9 \times 10^{11}$ G which is typical of accretion-powered pulsars (see Coburn et al. 2002). This magnetic field value is consistent with the previously suggested cyclotron lines around ∼10–20 keV of the source (Coburn et al. 2006). Galactic coordinates ($l = 332.^{\circ}779\,925$, $b = -2.^{\circ}002\,751$) and this distance estimate also imply that the source is on the rim of the Milky Way.

Fig. 2 shows that pulses from *Swift* J1626.6−5156 do not cease even after ∼1200 d from the outburst. This indicates that the source still accretes matter without any significant changes in the accretion geometry.

From Table 1 and Fig. 4, we see that the minimum n_H value is about 10^{22} cm^{-2}. We find that this value is consistent with the n_H estimates obtained from H I maps (Dickey & Lockman 1990; Kalberla et al. 2005).

In Fig. 4 we find that the power-law index is anticorrelated with the X-ray flux. This indicates that the spectrum becomes softer with a decreasing X-ray flux, which is expected and may be interpreted as a consequence of changes in mass accretion rate without a need for an accretion geometry change (Meszaros et al. 1983; Harding et al. 1984). Similar anticorrelation was also found for 2S 1417−62 (Inam et al. 2004) and SAX J2103.5+4545 (Baykal et al. 2007). Fig. 4 also reveals that hydrogen column density is correlated with the X-ray flux. This correlation was also seen in 2S 1417−62 and was thought to be due to the fact that matter concentration around the neutron star should be related to the mass accretion rate in Be/X-ray pulsar systems (Inam et al. 2004).

ACKNOWLEDGMENTS

We acknowledge the support by the research project TBAG 109T748 of the Scientific and Technological Research Council of Turkey (TÜBİTAK).

REFERENCES

Baykal A., Stark M., Swank J., 2002, ApJ, 569, 903
Baykal A., Inam S. C., Stark M. J., Heffner C. M., Erkoca A. E., Swank J. H., 2007, MNRAS, 374, 1108
Baykal A., Gogus E., Inam S. C., 2010, ApJ, 711, 1306
Bildsten L. et al., 1997, ApJS, 113, 367
Coburn W. et al., 2000, ApJ, 543, 351
Coburn W., Heindl W. A., Rothschild R. E., Gruber D. E., Kreykenbohm I., Wilms J., Kretschmar P., Staubert R., 2002, ApJ, 580, 394
Coburn W., Pottschmidt K., Rothschild R., Kretschmar P., Kreykenbohm I., Wilms J., McBride V., 2006, AAS/High-Energy Astrophys. Division, 9, 170
Dai H.-L., Li X.-D., 2006, A&A, 451, 581
DeCesar M. E., Pottschmidt K., Wilms J., 2009, Astron. Telegram, 2036
Deeter J. E., Boynton P. E., 1985, in Hayakawa S., Nagase F., eds, Proc. Inuyama Workshop Timing Studies X-ray Sources. Nagoya Univ., Nagoya, p. 29
Dickey J. M., Lockman F. J., 1990, ARA&A, 28, 215
Finger M. H., Wilson R. B., Chakrabarty D., 1996a, A&AS, 120, 209
Finger M. H., Wilson R. B., Harmon B. A., 1996b, ApJ, 459, 288
Finger M. H., Bildsten L., Chakrabarty D., Prince T. A., Scott D. M., Wilson C. A., Wilson R. B., Zhang S. N., 1999, ApJ, 517, 449
Garmire G. P., Bautz M. W., Fort P. G., Nousek J. A., Ricker G. R., 2003, Proc. SPIE, 4851, 28
Ghosh P., 1993, in Holt S. S., Day C. S., eds, The Evolution of X-ray Binaries. American Inst. Phys., New York, p. 439
Ghosh P., Lamb F. K., 1979, ApJ, 234, 296
Harding A. K., Kirk J. G., Galloway D. J., Meszaros P., 1984, ApJ, 278, 369
in't Zand J. J. M., Corbet R. H. D., Marshall F. E., 2001, ApJ, 553, L165
Inam S. C., Baykal A., Scott D. M., Finger M., Swank J., 2004, MNRAS, 349, 173
Inam S. C., Townsend L. J., McBride V. A., Baykal A., Coe M. J., Corbet R. H. D., 2009, MNRAS, 395, 1662
Jahoda K., Swank J. H., Giles A. B., Stark M. J., Strohmayer T., Zhang W., Morgan E. H., 1996, Proc. SPIE, 2808, 5
Kalberla P. M. W., Burton W. B., Hartmann D., Arnal E. M., Bajaja E., Morras R., Pöppel W. G. L., 2005, A&A, 440, 775
Lamb F. K., Pethick C. J., Pines D., 1973, ApJ, 184, 271
Li J., Wickramasinghe D. T., 1998, MNRAS, 300, 1015
Markwardt C. B., Swank J. H., 2005, Astron. Telegram, 679
Meszaros P., Harding A. K., Kirk J. G., Galloway D. J., 1983, ApJ, 266, L33
Negueruela I., Marco A., 2006, Astron. Telegram, 739
Palmer D., Barthelmy S., Cummings J., Gehrels N., Kennea J., Krimm H., Markwardt C. B., Tueller J., 2005, Astron. Telegram, 678
Parmar A. N., White N. E., Stella L., 1989, ApJ, 184, 271
Pringle J. E., Rees M. J., 1972, A&A, 21, 1
Rea N., Testa V., Israel G. L., Antonelli A., Jonker P., Belloni T., Campana S., Stella L., 2006, Astron. Telegram, 713
Reig P., Belloni T., Israel G. L., Campana S., Gehrels N., Homan J., 2008, A&A, 485, 797
Scott D. M., Finger M. H., Wilson R. B., Koh D. T., Prince T. A., Vaughan B. A., Chakrabarty D., 1997, ApJ, 488, 831
Torkelsson U., 1998, MNRAS, 298, 55
Wang Y.-M., 1987, A&A, 183, 257
White N. E., Swank J. H., Holt S. S., 1983, ApJ, 270, 711
Wilms J., Nowak M. A., Dove J. B., Fender R. P., di Matteo T., 1999, ApJ, 522, 460
Wilson C. A., Finger M. H., Coe M. J., Laycock S., Fabregat J., 2002, ApJ, 570, 287

This paper has been typeset from a TEX/LATEX file prepared by the author.